# Prospects for Time-of-Flight PET using LSO Scintillator*

W. W. Moses, *Senior Member, IEEE*, and S. E. Derenzo, *Senior Member, IEEE*
Lawrence Berkeley National Laboratory, University of California, Berkeley, CA 94720 USA

## *Abstract*

We present measurements of the timing properties of lutetium orthosilicate (LSO) scintillator crystals coupled to a photomultiplier tube (PMT) and excited by 511 keV photons. These crystals have dimensions suitable for use in PET cameras (3x3x30 $mm^3$). Coincidence timing resolution of 475 ps fwhm is measured between detectors utilizing two such crystals, significantly worse than the 300 ps fwhm predicted based on first principles for small crystals and measured in 3 mm cubes. This degradation is found to be caused by the scintillation light undergoing multiple reflections at quasi-random angles within the scintillator crystal, which has two effects. First, it slows down the effective information propagation speed within the crystal (to an effective $\hat{n}$=3.9–5.3). Since the incident annihilation photon travels with $n$=1, information from interactions at different depths arrives at the PMT with different time delays. Second, the random nature of the reflection angles (and path lengths) introduce dispersion and so a 10%–90% rise time of 1 ns to the optical signal.

## I. INTRODUCTION

It has long been recognized that the inclusion of time-of-flight (TOF) information would improve the performance of PET (positron emission tomography) [1-4]. As shown in Figure 1, by measuring the difference of the arrival times of the 511 keV photons a PET camera could restrict the position of the positron emission to a subsection of the chord (the line segment joining the two scintillation crystals that detect the 511 keV photons). As these photons travel at $c$=3x$10^8$ m/s, a coincidence timing resolution of 500 ps fwhm restricts the positron position to a 7.5 cm fwhm length. This restriction is much coarser than the ~4 mm localization afforded by the size of the scintillation crystals, so the net result is not to improve spatial resolution but to assist the tomographic reconstruction algorithm and reduce the statistical noise in the reconstructed image. The variance reduction factor is approximately equal to the typical linear dimension of the emission source divided by the length of TOF localization distance [5].

Several time-of-flight PET cameras have been built using $BaF_2$ and CsF scintillator crystal and typically obtain 500 ps fwhm coincidence timing resolution [6-8]. When imaging cross sections of the human body (typical linear dimension of 20–30 cm), they should produce images whose statistical noise is comparable to that obtained with 2.5–3.75 times the number of events with non-TOF PET cameras. However, these TOF PET cameras have not seen widespread usage because of other compromises inherent in these systems. Specifically, the ultraviolet emissions of $BaF_2$ require the use of relatively expensive quartz windowed photomultiplier tubes and the lower density and photoelectric fraction (compared to BGO or bismuth germanate, the most commonly used scintillator for PET) exacerbates the penetration of the 511 keV photons into the detector ring before they interact, degrading the spatial resolution.

The recently discovered scintillator LSO (cerium activated lutetium orthosilicate, or $Lu_2SiO_5$:Ce) [9] appears to have the potential to provide time-of-flight information without sacrificing other performance characteristics necessary for PET. It has a 1.2 cm attenuation length and 34% photoelectric fraction, giving it the ability to stop the annihilation photons in a short distance. Its 20,000–30,000 photon/MeV luminosity gives it good energy resolution and 40 ns decay time gives it minimal dead time. These qualities are generally more favorable for PET than those of BGO, and so LSO has been proposed for use in a wide variety of non-TOF PET detector module designs.

In addition, the LSO luminosity and decay time figures imply an initial scintillation photon intensity of ~250–375 photons/ns for a 511 keV energy deposit, or one photoelectron every 27–40 ps, assuming a 50% light collection efficiency and 20% quantum efficiency. This is nearly as high as the ~1,300 photons/ns for a 511 keV energy deposit rate produced by $BaF_2$, so reasonably accurate timing can be expected from LSO. In fact, 160 ps fwhm time response has been obtained from a single LSO crystal when >1 MeV energy is deposited in the crystal [10, 11].

However, the timing properties of a scintillator are known to depend on both the energy deposited in the crystal and the shape of the scintillation crystal. The results in [10, 11] were obtained with a 4x5x14.5 $mm^3$ LSO crystal coupled on the 5x14.5 $mm^2$ surface [12] and excited by 1.3 MeV photons — neither the size nor the energy is appropriate for PET. Thus, this work explores the timing resolution possible under

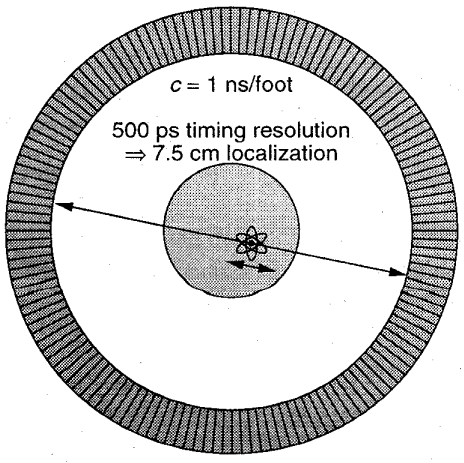


Figure 1. Time-of-Flight PET Camera. Annihilation photons are detected by a ring of scintillation crystals. With a conventional PET camera, this localizes the position of the positron to the line segment joining the two crystals. With a TOF PET camera, the arrival time difference is used to further restrict the position.

* This work was supported in part by the U.S. Department of Energy under Contract No. DE-AC03-76SF00098, and in part by Public Health Service Grant No. P01-HL8605-26 from the National Heart, Lung, and Blood Institute of the National Institutes of Health.

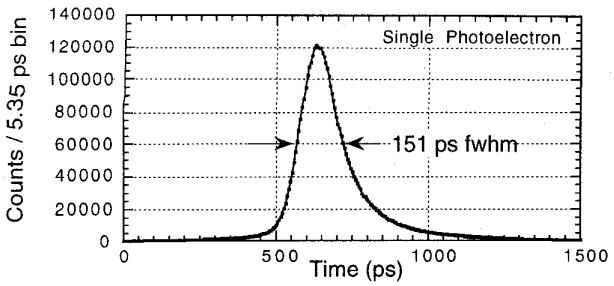


Figure 2. Measured single photoelectron transit time jitter.

conditions appropriate for PET, specifically a 3x3x30 $mm^3$ LSO crystal coupled to the photomultiplier tube on the 3x3 $mm^2$ end and excited with 511 keV photons. We measure the coincidence timing as a function of crystal length and surface treatment and also explore the factors that limit the timing by measuring the rise time of the optical signal emitted from the crystals.

## II. Apparatus

Four different crystal geometries are measured. All are 3x3 $mm^2$ in cross section and 3, 10, 20, or 30 mm in length. The 3 mm cubes have a mechanical polish on all six faces, while both polished and chemically etched [13] (on all six faces) surface finishes are explored for crystals with the three longer lengths. For each size and surface finish, two crystals are produced and tested. Approximately 75% of the crystals come from one boule of LSO and the remaining crystals from another. While the statistics are small, no boule to boule differences are observed.

For the coincidence timing experiments, two Hamamatsu R-5320 PMTs operated at –2400 V are used. These PMTs are 26 mm diameter (a size compatible with common PET detector designs) and specified by the manufacturer to have a 700 ps rise time and 160 ps fwhm single photoelectron transit time jitter [14]. Timing signals are generated from the PMT outputs with a Tennelec TC-454 constant fraction discriminator with its threshold set to trigger on single photoelectrons and a fraction of 0.3. These timing signals start and stop a time-to-amplitude converter, whose output is digitized and recorded by a computer. In addition, the output from each PMT is sent to a shaper amplifier (1 μs time constant) and the amplifier outputs sent to discriminators whose thresholds are set to an equivalent of 250 keV. Data from an event is only recorded when there is a loose (200 ns) time coincidence between these "slow" signals.

For the rise time measurements, the crystals are excited with a 35 ps wide pulse of x-rays. These x-rays are produced by a light-excited x-ray source whose x-ray output intensity is proportional to the incident light intensity, modulo a 35 ps time dispersion. The system is the same as is described in [15, 16] except that the x-ray intensity and time resolution are significantly improved by replacing the diode laser that excites the system with a titanium-doped sapphire laser. Fluorescent photons are detected with a microchannel plate photomultiplier tube and converted into timing pulses and digitized using the same electronics as above (without the "slow" coincidence gate). The impulse response of the system is 60 ps fwhm, and

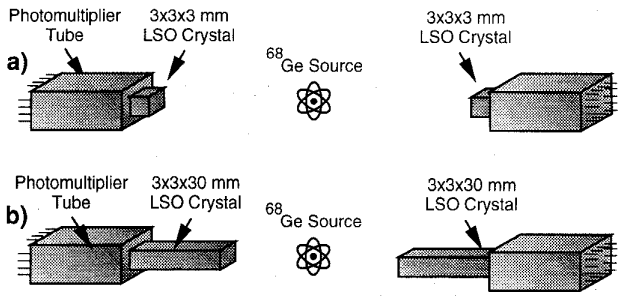


Figure 3. Measurement geometry for coincidence timing.

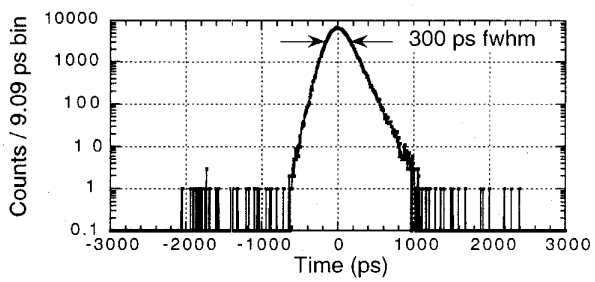


Figure 4. Coincidence timing with 3 mm LSO cubes.

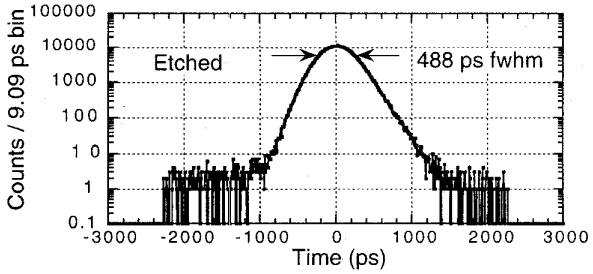


Figure 5. Coincidence timing with 3x3x30 $mm^3$ LSO crystals.

the scintillation photon arrival time spectrum is determined using the delayed coincidence method [17].

The single photoelectron transit time jitter of the photomultiplier tube is measured using the same electronics as used in the paragraph above, except the R-5320 photomultiplier tube is excited directly by the (attenuated) laser beam. The results, shown in Figure 2, indicate a 151 ps fwhm transit time jitter, consistent with the manufacturer's value of 160 ps fwhm [14].

## III. Coincidence Timing

The coincidence timing for 3 mm LSO cubes is measured with the geometry shown in Figure 3a. The results, shown in Figure 4, indicate a coincidence timing resolution of 300 ps fwhm. This value agrees with the 320 ps value derived from the 160 ps fwhm single channel timing resolution reported in [10, 11]. To derive the 320 ps value from the 160 ps measurement, we scale by the square root of the ratio of the gamma ray energies (to compensate for the differing signal magnitudes) and by the square root of 2 (to convert single-channel timing to coincidence timing). The 3 mm cubes are replaced with 3x3x30 $mm^3$ LSO crystals, as shown in Figure 3b, and the resulting coincidence timing distribution (with etched crystals) is shown in Figure 5. In this

Table 1. Timing resolution versus surface finish and length for a 3 mm LSO cube in coincidence with a 3x3xZ mm$^3$ LSO crystal, where Z=10, 20, or 30 mm. Note that two crystals of each length and finish are measured.

| | Surface Treatment | | | |
|---|---|---|---|---|
| Length | Etched #1 | Etched #2 | Polished A | Polished B |
| 10 mm | 317 ps | 327 ps | 324 ps | 309 ps |
| 20 mm | 391 ps | 403 ps | 385 ps | 385 ps |
| 30 mm | 455 ps | 443 ps | 397 ps | 415 ps |

configuration, the coincidence timing resolution is increased to 488 ps fwhm with etched crystals and 458 ps fwhm with polished crystals.

Thus, we observe that the coincidence time resolution depends on the length of the crystal and the possibly on the surface finish. To further characterize this dependence, we replace one of the crystals in Figure 3b with a 3 mm LSO cube and the other with a "test" crystal of dimensions 3x3xZ mm$^3$ (where Z = 10, 20, or 30 mm and the surface finish is either etched or polished) and measure the coincidence timing resolution. The results, summarized in Table 1, indicate that the timing resolution progressively degrades with increasing length. It also indicates that while the surface finish does not appears to play a large role, polished crystals may have better timing resolution for long (Z≥20 mm) crystals.

## IV. Propagation Time Measurements

One possible explanation for the degradation of the coincidence time resolution with increasing crystal length involves propagation time. As Figure 6 demonstrates, information (in the form of a 511 keV photon) travels at the velocity of light ($c$) from the radioactive source to the point where it interacts within the scintillator crystal. After interacting, the information (in the form of scintillation photons) travels at the velocity $c/\hat{n}$ (where $\hat{n}$ is the effective index of refraction) from the interaction point to the PMT. Thus, interaction at different positions in the scintillation will lead to differences in the time taken for information to propagate from the radioactive source to the PMT, increasing the coincidence resolving time. The magnitude of this effect is proportional to crystal length, consistent with the data in Table 1.

To test this hypothesis we use the geometry shown in Figure 7. An electronically collimated beam of 511 keV photons (formed by the PMT on the left and the positron emitting source) excites a small region (typically 2.5 mm fwhm) of the 3x3x30 mm$^3$ LSO crystal coupled to the PMT on the right. The scintillator crystal and PMT on the right can move parallel to the long axis of the crystal, so the distance of this excitation position from the PMT face can be varied. Since the length of the cable connecting this PMT to the subsequent electronics is not changed as it moves, the propagation time from the PMT to the electronics is constant.

At each excitation depth, the center (and fwhm) of the coincidence timing distribution is measured, and is plotted as a function of excitation depth in Figure 8. For all cases, a coincidence timing resolution of 375±35 ps fwhm is measured. The slope of this line gives an effective propagation velocity which, when compared to the speed of light in vacuum ($c$),

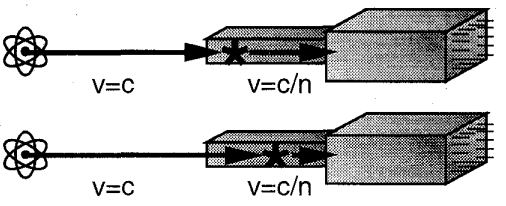


Figure 6. Propagation Time Differences. In the sketches above, information travels at velocity $c$ from the radioactive source to the interaction point in the scintillator crystal, and at velocity $c/n$ from the interaction point to the photomultiplier tube. Because of this, the time that it takes signal to travel from the source to the photomultiplier tube depends on the interaction position even though the total distance is the same.

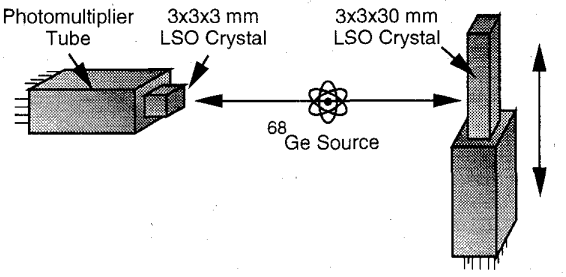


Figure 7. Geometry used to measure the information propagation speed within then crystal. The PMT (and scintillator crystal) at the right move parallel to the long edge of the page. The cable length is kept constant, so that the information propagation time from the PMT to the electronics is independent of this position.

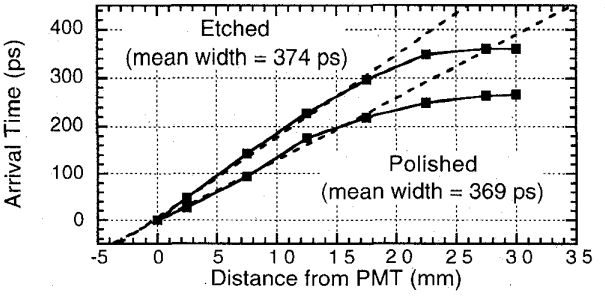


Figure 8. Center of coincidence timing distribution as a function of excitation depth using the geometry shown in Figure 7.

gives an effective index of refraction $\hat{n}$. Figure 8 shows that the $\hat{n}$ for the etched and polished crystals is 5.3 and 3.9 respectively. This increase over the nominal index of 1.82 for LSO is probably due to multiple reflections within the crystal increasing the path length. We attribute the flattening of the curves at distances greater than 20 mm to the fact that most of the light that ends up exciting the PMT is either originally emitted directly toward or directly away from the PMT. When the excitation position is close to the PMT, only the "direct" light is likely to trigger the timing electronics, as the "opposite" light must travel to the far end of the crystal, then reflect and again travel the length of the crystal, delaying it significantly. As the excitation position moves farther from the PMT, the difference between arrival times of the "direct" and "opposite" light decreases until the two merge (in time), at which point the electronics triggers sooner because the optical photon rate is higher and the system triggers on the first photon that it detects.

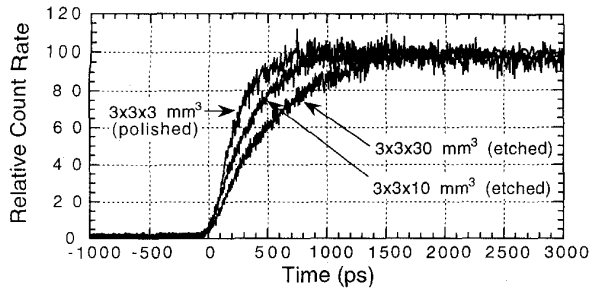


Figure 9. Scintillation photon arrival time distributions for 3x3xZ mm$^3$ etched LSO crystals uniformly illuminated by x-rays.

## V. Rise Time Measurements

Another potential cause for the degraded coincidence time resolution with increasing length is the rise time of the optical signal. As shown in [11, 18, 19], even a fairly small (~500 ps) rise time significantly reduces the initial photon rate and significantly degrades the theoretically achievable timing resolution. In order to investigate whether the effective rise time is affected by crystal length, we measure the arrival time distribution of etched and polished LSO crystals of dimensions 3x3xZ mm$^3$ (where Z = 3, 10, 20, or 30 mm) that are uniformly illuminated with x-rays. The scintillation photon arrival time distributions for several length etched crystals shown in Figure 9 indicate that there are significant rise time differences. Table 2 displays this dependence quantitatively (calculated as 10%–90% rise times) for the various crystal geometries. As in Table 1, the rise time progressively increases with increasing length. Table 2 also indicates that while the surface finish does not appear to play a large role, polished crystals may have a faster rise time than etched crystals for long (Z≥20 mm) crystals but slower rise time than etched crystals for short (Z≤20 mm) crystals.

Finally, we would like to understand the origin of this rise time. One possibility is that the increase in rise time observed in Figure 9 and Table 2 is due to the propagation time delays observed in Section IV. In a simplified model, all scintillation photons emitted from a single depth in the crystal take exactly the same time to travel to the photocathode. Thus with point excitation one would observe the intrinsic LSO rise time. Since the travel time depends on excitation depth and the scintillator crystals are uniformly excited by x-rays, averaging over multiple excitations manifests itself as an apparent rise time. An alternate hypothesis is that even when scintillation photons are emitted from a single position, they undergo a large number of quasi-random internal reflections within the crystal (independent of the excitation position) before exiting the crystal and being detected. The variability in path length (which would depend on the length and surface finish) implies time dispersion that increases the observed rise time, even though the intrinsic rise time of LSO is unaffected.

To try to distinguish these two hypotheses, we repeat the rise time measurement but excite at a single 3 mm long section of an etched 3x3x30 mm$^3$ crystal located 20 mm from the exit face. A rise time similar to that of the 3 mm cube would indicate that propagation time delays are responsible for the rise time, while a rise time similar to the uniformly illuminated crystal would indicate that dispersion

Table 2. 10%–90% rise time versus surface finish and length for 3x3xZ mm$^3$ LSO crystal, where Z=3, 10, 20, or 30 mm. Note that two crystals of each type are measured.

| | Surface Treatment | | | |
|---|---|---|---|---|
| Length | Etched #1 | Etched #2 | Polished A | Polished B |
| 3 mm | | | 484 ps | 465 ps |
| 10 mm | 657 ps | 693 ps | 879 ps | 921 ps |
| 20 mm | 967 ps | 751 ps | 1021 ps | 1094 ps |
| 30 mm | 1175 ps | 1204 ps | 858 ps | 866 ps |

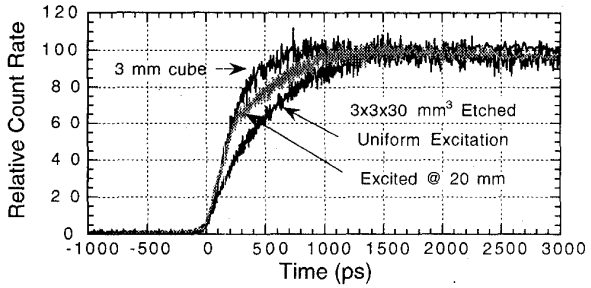


Figure 10. Scintillation photon arrival time distribution for a 3x3x30 mm$^3$ etched LSO crystal illuminated with x-rays 20 mm depth compared to those from uniformly illuminated crystals.

caused by multiple reflections is the culprit. The data, shown in Figure 10, is somewhat ambiguous. At early times, the data follows that of the 3 mm cube, while at later times it becomes more similar to the uniformly excited crystal. However, the coincidence timing is most influenced by the earliest portions of the rise time distribution. As the earliest portions of the rise time distribution are most similar to that of the 3 mm cube, it is likely that propagation delay is largely responsible for the increased rise time.

## VI. Discussion

While very good (300 ps fwhm) coincidence timing is obtained with small LSO crystals, the timing resolution is degraded to ~475 ps fwhm when the 30 mm long crystals necessary for efficient detection of 511 keV photons are used. The cause of this degradation is probably due to the fact that scintillation photons often undergo multiple reflections within the crystal before they exit and are detected by the PMT. These multiple reflections have two main effects: to decrease the velocity at which information propagates through the crystal (due to the increased path length that the scintillation photons must travel) and to add time dispersion (due to variations in path lengths traveled by photons emitted from the same position). The magnitude of both of these effects will increase with increasing crystal size.

The effect caused by propagation time can be eliminated if the interaction depth within the crystal is known — the coincidence time resolution is improved from 458 ps (as reported in Section III) to 369 ps (shown in Figure 8) when an etched crystal is excited at a fixed depth rather than throughout the crystal. Measurement of depth-of-interaction is also desirable in order to reduce a spatial resolution artifact known as radial elongation and there are several proposed

LSO-based designs that include this capability. It may be possible that such designs could also measure time-of-flight.

The concept of adding time-of-flight measurement to an existing detector design suggests a final point, which is that a single 3x3x30 $mm^3$ crystal does not fully represent a PET detector module. While many PET detector modules utilize similarly sized crystals, virtually all incorporate some sort of multiplexing scheme so that the number of crystals read out is significantly (10–100 times) larger than the number of photomultiplier tubes. These multiplexing schemes are usually optical in nature and so entail longer path lengths than those for a single crystal, and this increase in path length is likely to degrade the timing. Furthermore, the optical signal from a single crystal is often shared between multiple photomultiplier tubes, and will require significant effort to avoid introducing PMT dependent time shifts when extracting the timing information from the separate signals.

## VII. Conclusion

We have shown that while 300 ps fwhm coincidence time resolution is achieved with 3 mm cubes of LSO excited with annihilation photons, the timing is degraded to ~475 ps fwhm when 3x3x30 $mm^3$ LSO crystals are used. Nonetheless, this 475 ps fwhm resolution is sufficient to reduce the variance in reconstructed PET images by a factor of two and so would be worthwhile to incorporate into PET scanners. The degradation observed in the longer length crystals is due to two factors: finite propagation time of information through the scintillator crystal and time dispersion due to multiple reflections within the crystal. The former effect (which is probably the dominant one) can be reduced significantly by a correction based on the measured interaction position within the crystal. However, both of these effects are likely to be exacerbated by the optical decoding schemes commonly used in PET detector modules to read out more than one crystal pet PMT. Therefore, more study on the magnitude of these effects in more realistic PET detector module designs is necessary.

## VIII. Acknowledgment

We would like to thank Dr. R. Huesman of Lawrence Berkeley National Laboratory for many useful discussions. This work was supported in part by the Director, Office of Energy Research, Office of Biological and Environmental Research, Medical Applications and Biophysical Research Division of the U.S. Department of Energy under contract No. DE-AC03-76SF00098 and in part by the National Institutes of Health, National Heart, Lung, and Blood Institute under grant No. P01-HL8605-26. Reference to a company or product name does not imply approval or recommendation by the University of California or the U.S. Department of Energy to the exclusion of others that may be suitable.

## XI. References

[1] H. O. Anger, "Survey of radioisotope cameras," *Trans. ISA*, vol. 5, pp. 311–334, 1966.

[2] G. L. Brownell, C. A. Burnham, S. Wilenski, et al., "New developments in positron scintigraphy and the application of cyclotron-produced positron emitters," in *Medical Radioisotope Scintigraphy*: Proceedings of a Conference, Salzburg, August 6-15, 1968, Vienna, I.A.E.A., 1969, pp. 163.

[3] R. Allemand, C. Gresset, and J. Vacher, "Potential advantages of a Cesium Fluoride scintillator for a time-of-flight positron camera," *J. Nucl. Med.*, vol. 21, pp. 153-155, 1980.

[4] N. A. Mullani, D. C. Ficke, R. Hartz, et al., "System design of fast PET scanners utilizing time-of-flight," *IEEE Trans. Nucl. Sci.*, vol. NS-28, pp. 104-107, 1981.

[5] T. F. Budinger, "Time-of-flight positron emission tomography: Status relative to conventional PET," *J. Nucl. Med.*, vol. 24, pp. 73-78, 1983.

[6] R. Gariod, R. Allemand, and E. Cormoreche. The "LETI" positron tomograph architecture and time of flight improvements. Proceedings of The International Workshop on Time-of-Flight Positron Tomography, IEEE Catalog No 82CH1719-3, 1982.

[7] N. A. Mullani, J. Gaeta, K. Yerian, et al., "Dynamic imaging with high resolution time-of-flight PET camera - TOFPET I," *IEEE Trans. Nucl. Sci.*, vol. NS-31, pp. 609-613, 1984.

[8] T. K. Lewellen, A. N. Bice, R. L. Harrison, et al., "Performance measurements of the SP3000/UW time-of-flight positron emission tomograph," *IEEE Trans. Nucl. Sci.*, vol. NS-35, pp. 665-669, 1988.

[9] C. L. Melcher and J. S. Schweitzer, "Cerium-doped lutetium orthosilicate: a fast, efficient new scintillator," *IEEE Trans. Nucl. Sci.*, vol. NS-39, pp. 502-505, 1992.

[10] T. Ludziejewski, M. Moszynska, M. Moszynski, et al., "Advantages of LSO scintillator in nuclear physics experiments," *IEEE Trans. Nucl. Sci.*, vol. NS-42, pp. 328–336, 1995.

[11] M. Moszynski, T. Ludziejewski, D. Wolski, et al., "Timing properties of GSO, LSO and other Ce doped scintillators," *Nucl. Instr. Meth.*, vol. A 372, pp. 51-58, 1996.

[12] M. Moszynski, Personal communication, 1998.

[13] K. Kurashige, Y. Kurata, H. Ishibashi, et al., "Surface polishing of GSO scintillator using chemical process," *IEEE Trans. Nucl. Sci.*, vol. NS-45, pp. 522-524, 1998.

[14] Hamamatsu Photonics, *Photomultiplier tubes and assemblies for scintillation counting and high energy physics*, p. 16–17, 1998.

[15] S. C. Blankespoor, S. E. Derenzo, W. W. Moses, et al., "Characterization of a pulsed x-ray source for fluorescent lifetime measurements," *IEEE Trans. Nucl. Sci.*, vol. NS–41, pp. 698–702, 1994.

[16] W. W. Moses, S. E. Derenzo, M. J. Weber, et al., "Scintillator characterization using the LBL pulsed x-ray facility," *Rad. Meas.*, vol. 24, pp. 337–341, 1995.

[17] L. M. Bollinger and G. E. Thomas, "Measurement of the time dependence of scintillation intensity by a delayed-coincidence method," *Rev. Sci. Instr.*, vol. 32, pp. 1044–1050, 1961.

[18] L. G. Hyman, R. M. Schwarcz, and R. A. Schluter, "Study of high speed photomultiplier tube systems," *Rev. Sci. Instr.*, vol. 35, pp. 393–406, 1964.

[19] L. G. Hyman, "Time resolution of photomultiplier tube systems," *Rev. Sci. Instr.*, vol. 36, pp. 193–196, 1965.